

Oxidation of Titanium-Decorated Single-Walled Carbon Nanotubes and Subsequent Reduction by Lithium

Ich C. Tran,^{*,†} Roberto Félix,^{†,‡} Marcus Bär,^{†,‡} Lothar Weinhardt,^{†,§} Yufeng Zhang,[†] and Clemens Heske^{*,†}

Department of Chemistry, University of Nevada Las Vegas (UNLV), Las Vegas, Nevada 89154-4003, Solar Energy Research, Helmholtz-Zentrum Berlin für Materialien und Energie GmbH, Hahn-Meitner-Platz 1, D-14109 Berlin, Germany, and Experimentelle Physik II, Universität Würzburg, Am Hubland, D-97074 Würzburg, Germany

Received December 30, 2009; E-mail: citran@unlv.nevada.edu; heske@unlv.nevada.edu

Abstract: The chemical surface structure of Ti-decorated single-walled carbon nanotubes (SWNTs) is studied. X-ray photoelectron spectra show that Ti adatoms on the SWNT surface oxidize even under ultra-high-vacuum conditions, presenting a serious obstacle for the use of Ti-decorated SWNTs for hydrogen storage. A subsequent deposition of Li can, however, reduce the degree of Ti oxidation, “liberating” Ti atoms for the interaction with hydrogen molecules in hydrogen storage applications.

1. Introduction

Carbon nanomaterials, in particular fullerenes and carbon nanotubes, have been considered as candidate materials for hydrogen storage.^{1,2} Recent experimental investigations using atomic hydrogen have shown a promising hydrogen storage capacity of 5.1 wt % for single-walled carbon nanotubes (SWNTs).^{3,4} Nevertheless, experiments have so far failed to show absorption of H_2 molecules on pure carbon nanotube structures exceeding a storage capacity of 1 wt %.^{5–7} It is clear that without considerable improvement SWNTs will not meet practical targets for hydrogen storage applications.

Theoretical predictions suggest that the coating of SWNTs with a transition metal (e.g., Ti) might enhance the hydrogen storage capability of SWNTs, as each Ti atom can potentially bind up to four hydrogen molecules.⁸ The binding mechanism is explained by a unique hybridization between the orbitals of the Ti adatoms and those of the SWNT C atoms, which facilitates the dissociation of, and bonding with, H_2 molecules. Previous experiments by Zhang et al. showed that it is indeed possible to uniformly coat carbon nanotubes with Ti atoms without metal segregation.⁹ None of the publications, however, address the effects of an “unintentional” presence of other elements, such as oxygen species, and their influence on the

hydrogen binding behavior. It is well known that metallic Ti, due to its chemically reactive nature, can easily be oxidized by interactions with oxygen and/or oxygen compounds, such as CO_x , NO_x , and water,^{10–12} which result in the formation of titanium oxides and/or hydroxides. It has also been found that metallic Ti rapidly reacts with residual gas even in ultra-high vacuum (UHV).¹³ In fact, Ti sublimation pumps are routinely used as very effective vacuum pumps in the UHV regime. This “natively” formed oxide/hydroxide coating on the deposited Ti can therefore be an obstacle for a controlled surface modification of carbon nanomaterials and might explain why experimental attempts to use Ti-coated carbon nanomaterials as hydrogen storage materials have so far not been successful.

In past surface science studies, high-temperature heat treatment and ion bombardment techniques have been regularly used to modify, reduce, or remove the titanium oxide/hydroxide surface layer.¹² Furthermore, Henningsson et al. have shown that titanium dioxide (anatase) can be reduced to lower oxidation states by the interaction with lithium in UHV, which leads to the formation of Li_xTiO_2 phases.^{14,15} In this paper, we thus first present an experimental study of the oxidation behavior of Ti-decorated SWNT by X-ray photoelectron spectroscopy (XPS). We will show that Ti-decorated carbon nanotubes are very susceptible to oxidation even under UHV conditions. Then, we also explore the possibility of using Li as a getter agent to reduce the degree of Ti oxidation on SWNTs, thus liberating Ti atoms for the potential adsorption of hydrogen molecules.

[†] UNLV.

[‡] Helmholtz-Zentrum Berlin für Materialien und Energie GmbH.

[§] Universität Würzburg.

- (1) Dillon, A. C.; Jones, K. M.; Bekkedahl, T. A.; Kiang, C. H.; Bethune, D. S.; Heben, M. J. *Nature* **1997**, *386*, 377.
- (2) Cheng, H. M.; Yang, Q. B.; Liu, C. *Carbon* **2001**, *39*, 1447–1454.
- (3) Nikitin, A.; Ogasawara, H.; Mann, D.; Denecke, R.; Zhang, Z.; Dai, H.; Cho, K.; Nilsson, A. *Phys. Rev. Lett.* **2005**, *95*, 225507.
- (4) Nikitin, A.; Li, X.; Zhang, Z.; Ogasawara, H.; Dai, H.; Nilsson, A. *Nano Lett.* **2008**, *8*, 162–167.
- (5) Zuttel, A. *Mater. Today* **2003**, *6*, 24.
- (6) Tibbetts, G. G.; Meisner, G. P.; Olk, C. H. *Carbon* **2001**, *39*, 2291.
- (7) Centrone, A.; Brambilla, L.; Zerbi, G. *Phys. Rev. B* **2005**, *71*, 245406.
- (8) Yildirim, T.; Ciraci, S. *Phys. Rev. Lett.* **2005**, *94*, 175501.
- (9) Zhang, Y.; Franklin, N. W.; Chen, R. J.; Dai, H. *Chem. Phys. Lett.* **2000**, *331*, 35–41.

- (10) Carley, A. F.; Chalker, P. R.; Rivieret, J. C.; Roberts, M. W. *J. Chem. Soc., Faraday Trans. 1* **1987**, *83*, 351–370.
- (11) Miller, S.; Berning, G. L. P.; Plank, H.; Roth, J. J. *Vac. Sci. Technol. A* **1997**, *15*, 2029–2034.
- (12) Mayer, J. T.; Diebold, U.; Madey, T. E.; Garfunkel, E. J. *Electron Spectrosc. Relat. Phenom.* **1995**, *73*, 1–11.
- (13) Polak, M.; Hefetz, M.; Mintz, M. H.; Dariel, M. P. *Surf. Sci.* **1983**, *126*, 739–744.
- (14) Henningsson, A.; Andersson, M. P.; Uvdal, P.; Siegbahn, H.; Sandell, A. *Chem. Phys. Lett.* **2002**, *360*, 85–90.
- (15) Richter, J. H.; Henningsson, A.; Karlsson, P. G.; Andersson, M. P.; Uvdal, P.; Siegbahn, H.; Sandell, A. *Phys. Rev. B* **2005**, *71*, 235418.

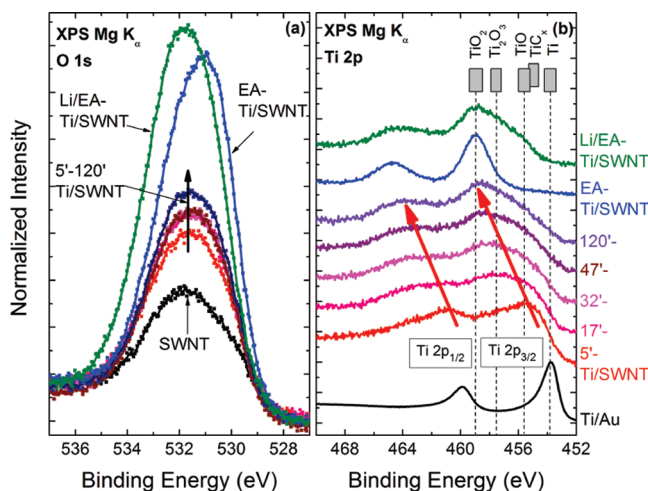


Figure 1. Evolution of O 1s (a) and Ti 2p (b) photoemission spectra of a SWNT/Au sample before (O 1s only) and after Ti deposition as a function of time in ultra-high vacuum (UHV), after air exposure (EA), and after subsequent in situ Li deposition. The O 1s spectra (raw data: dots) were smoothed (solid lines) and normalized to the intensity at 527 eV, while the Ti 2p spectra were normalized to their peak maximum and offset vertically. For comparison, the Ti 2p spectrum of a thick metallic Ti layer (deposited on a Au substrate) and the energetic position of the Ti 2p_{3/2} photoemission lines of different Ti reference compounds (gray boxes, from refs 10–12 and 18) are shown.

2. Experimental Section

Purified SWNT samples (Carbon Nanotubes, Inc., batch #P0288, “Super Pure” type with impurity and moisture content less than 5 wt %) were dispersed in dimethylformamide using an ultrasonic bath. Thin films of SWNTs were prepared by vacuum-drying a drop of the SWNTs dispersion on Au/Si substrates (Platypus Technologies). Deposition of Ti was performed under UHV (10^{-10} mbar range, up to 5×10^{-9} mbar during Ti deposition), using a Focus EFM-3 electron-beam evaporator operating at a flux-current of 100 nA from a 2.0 mm diameter Ti wire (Alfa Aesar, 99.99% purity). XPS measurements were performed in UHV (base pressure $\sim 1 \times 10^{-10}$ mbar) using Mg K α and Al K α radiation and a SPECS Phoibos 150MCD electron analyzer. After a detailed XPS investigation of the oxidation behavior in UHV, the Ti/SWNT/Au sample was exposed to ambient atmosphere (denoted as EA, “exposed to air”) for 30 min and reintroduced into the UHV chamber. Subsequently, the EA-Ti/SWNT/Au sample was decorated with Li from a carefully outgassed Li getter element (SAES; the pressure increased up to 5×10^{-8} mbar during Li evaporation). The effective thickness of the deposited Ti and Li metal layers was estimated by the attenuation of the SWNT/Au C 1s XPS peak (~ 1 and ~ 5 Å for 30 s deposition of Ti and Li, respectively), taking the inelastic mean free path of the C 1s photoelectrons in pure Ti and Li into account.¹⁶

3. Results and Discussion

Figure 1 shows the evolution of the (a) O 1s and (b) Ti 2p photoemission lines for the SWNT/Au sample before (O 1s only) and after Ti deposition. Spectra taken as a function of “storage” time in UHV, after exposing the Ti-deposited sample to air (EA), and after subsequent deposition of Li are also shown. In addition, the Ti 2p spectrum measured for a thick Ti layer on a Au substrate is plotted in Figure 1b for comparison (clearly showing the characteristic Doniach–Šunjić line shape of a metal). The O 1s signal for the SWNT/Au sample is due to

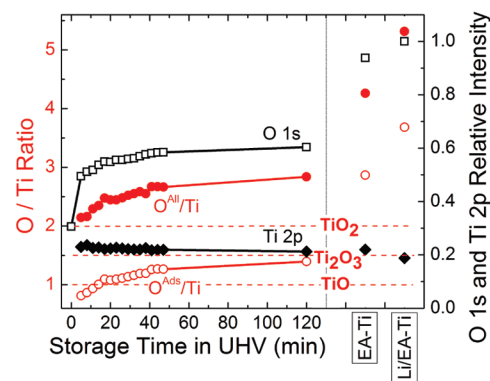


Figure 2. Evolution of the O 1s (open black squares) and Ti 2p (solid black diamonds) intensities (error bars are estimated to 5% before and 10% after air exposure) and of the O/Ti surface ratio as a function of UHV storage time after Ti deposition, after air exposure (EA), and after subsequent Li deposition. “O^{All}” (solid red circles) refers to the overall oxygen intensity, while “O^{Ads}” (open red circles) reflects the intensity of the additionally adsorbed oxygen only. The dashed lines indicate the expected O/Ti ratios for different nominal Ti oxide compositions.

oxygen species adsorbed on the surface of the SWNTs due to ambient exposure prior to Ti deposition.¹⁷ A detailed quantitative XPS analysis (not shown) shows that the oxygen content on the pristine SWNT sample is approximately 3.3 at. % of the overall volume probed in XPS.

A pronounced increase of the oxygen signal can be observed after Ti deposition, both initially and as a function of residence time in UHV (5 to 120 min). This indicates the adsorption (gettering) of additional oxygen species from the residual gas due to the high chemical reactivity of the Ti adatoms. Air exposure (EA) and Li adsorption lead to a further increase of the O 1s intensity and a shift in line position.

The interaction of Ti with adsorbed oxygen species is also evident from the evolution of the Ti 2p photoemission lines (Figure 1b). The first Ti 2p spectrum (measured 5 min after Ti deposition) shows a broad Ti 2p_{3/2} and Ti 2p_{1/2} spin–orbit doublet. A comparison with the metallic Ti/Au reference and corresponding literature data^{10–12,18} of different Ti species (shown by gray boxes in Figure 1b) suggests that the deposited Ti adatoms on SWNTs have formed Ti–C and/or Ti–O bonds (note that Ti is initially deposited in metallic form, as can be derived from the clearly metallic character of the Ti/Au reference spectrum). The detailed bonding environments of the Ti atoms will be discussed in conjunction with Figure 3.

As the storage time increases, the Ti 2p peaks broaden and their maxima gradually shift to higher binding energy (BE), as indicated by the red arrows. Comparison with the reference data suggests an increasing degree of oxidation with time, in agreement with the O 1s spectra in Figure 1a. This, in turn, suggests a continuous adsorption of oxygen species from the UHV residual gas. Air exposure (EA) leads to a pronounced, TiO₂-like spectrum, and subsequent Li deposition again leads to peak broadening, which will be analyzed in detail in Figure 4.

Figure 2 shows a quantitative analysis of the Ti and O peak areas derived from the spectra in Figure 1. First, we subtract a

(16) Tanuma, S.; Powell, C. J.; Penn, D. R. *Surf. Interface Anal.* **1993**, *21*, 165.

(17) Kuznestsova, A.; Popova, I.; Yates, J. T.; Bronikowski, M. J.; Huffman, C. B.; Kiu, J.; Smalley, R. E.; Hwu, H. H.; Chen, J. G. *J. Am. Chem. Soc.* **2001**, *123*, 10699.

(18) Moulder, J. W.; Stickle, W. F.; Sobol, P. E.; Bomben, K. D. In *Handbook of X-ray Photoelectron Spectroscopy*; Chastain, J., Ed.; Perkin-Elmer Corp., 1992.

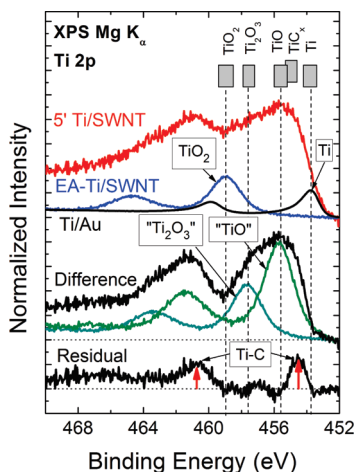


Figure 3. Ti 2p spectra of the Ti/SWNT sample after 5 min storage in UHV (top, red) and its decomposition into contributions from metallic Ti, various Ti oxides (TiO_2 , Ti_2O_3 , and TiO), and Ti–C bonds.

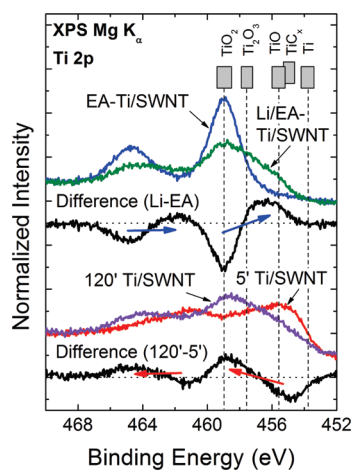


Figure 4. (Bottom) Ti 2p spectra of the Ti/SWNT sample after 5 and 120 min storage in UHV, together with their difference spectrum. (Top) Ti 2p spectra of the air-exposed Ti/SWNT sample before (“EA-Ti/SWNT”) and after (“Li/EA-Ti/SWNT”) Li deposition, together with their difference spectrum. Arrows indicate the shift of spectral weight due to oxidation and Li-induced reduction.

linear background and correct with the corresponding photoionization cross sections¹⁹ (since the BEs of the Ti 2p and O 1s photoelectrons are similar, the energy dependence of the analyzer transmission function and the inelastic mean free path can be neglected). The O 1s (open black squares) and Ti 2p (solid black diamonds) intensities (i.e., areas) are then shown as “relative intensity” (Figure 2, right scale) by arbitrarily setting the highest observed O 1s intensity (for the Li-deposited, air-exposed Ti/SWNT sample) to 1. It is evident that the increase of the O 1s intensity becomes less pronounced with increasing storage time, while the Ti 2p intensity shows a slight (but statistically significant) decrease. This can be explained by the increasing formation of a closed Ti oxide “cover”, resulting in the passivation of the chemically active Ti adatoms, slowing the adsorption of oxygen species from the residual gas.

In order to investigate the oxidation behavior of the deposited metallic Ti atoms in more detail, we now focus on the O/Ti surface ratio (Figure 2, left scale). Two different O/Ti ratios

were computed: $\text{O}^{\text{All}}/\text{Ti}$ (solid red circles in Figure 2) was computed using the integrated areas under the O 1s and Ti 2p photoemission peaks (corrected by the respective photoionization cross sections¹⁹). To compute $\text{O}^{\text{Ads}}/\text{Ti}$ (open red circles in Figure 2), the initial O 1s intensity (i.e., prior to Ti deposition) was subtracted from the overall O 1s intensity. While the computed $\text{O}^{\text{All}}/\text{Ti}$ ratio reflects a laterally averaged stoichiometry, $\text{O}^{\text{Ads}}/\text{Ti}$ reflects only the oxygen atoms newly adsorbed on the Ti-decorated SWNT. Note that a potential attenuation of the signal from initially adsorbed oxygen atoms by the deposited Ti atoms has only a minor impact on the computed $\text{O}^{\text{Ads}}/\text{Ti}$ ratio since the amount of deposited Ti is very small ($\sim 1 \text{ \AA}$ “thickness”).

For a comparison of the $\text{O}^{\text{Ads}}/\text{Ti}$ ratio with O/Ti ratios of Ti–O reference compounds, however, one has to take into account that a certain amount of the oxygen initially present on the SWNT/Au sample most likely will also form bonds to the deposited Ti. Hence, while the computed $\text{O}^{\text{All}}/\text{Ti}$ ratio will (strongly) overestimate the O/Ti stoichiometry, the $\text{O}^{\text{Ads}}/\text{Ti}$ ratio will underestimate it (both ratios count *all* Ti atoms; that is, they do not distinguish between Ti atoms in a Ti–O bond and those in a metallic or Ti–C-bonded environment; see discussion of Figure 3 below). Keeping that in mind, we compare the latter with the corresponding ratios for TiO, Ti_2O_3 , and TiO_2 and find that the average composition (of TiO_x) increases from $x = 0.82$ to $x = 1.4$ in the course of our UHV “exposure” (5 to 120 min). After air exposure, the O signal is significantly increased, while the Ti signal stays relatively constant (see individual data points at “EA-Ti” in Figure 2). The $\text{O}^{\text{All}}/\text{Ti}$ ratio is estimated at 4.3 and the $\text{O}^{\text{Ads}}/\text{Ti}$ ratio at 2.9. This indicates either a high degree of oxygen adsorption on the Ti atoms (i.e., beyond a TiO_2 stoichiometry) or, more likely, the deposition of oxygen-containing surface contaminants (e.g., water) in non-Ti-covered regions on the sample surface or on top of the TiO_2 . After Li deposition (see individual data points at “Li/EA-Ti” in Figure 2), the absolute intensity of O 1s is increased (due to additional oxygen adsorption), that of Ti 2p is decreased (due to attenuation by the Li or O atoms), and the O/Ti ratios are consequently further increased.

Next, we will discuss the partial Ti oxidation after five minutes of storage in UHV. The measured spectrum is shown at the top of Figure 3 (red). It is evident that multiple species contribute to the observed spectrum. For identification, we thus have used the following approach. (1) We observe significant spectral intensity at binding energies below 454 eV, which, based on the reference value (453.9 eV¹⁰) and our reference spectrum, is ascribed to metallic Ti. We have thus subtracted the Ti metal reference spectrum from the spectrum of the “5 min sample” after multiplying with the maximal possible factor that still gives a feasible (nondistorted, continuous, and non-negative) line shape below 454 eV for the residual spectrum (this metallic contribution is 8.0% of the overall spectral intensity). (2) We assume that the final stages of oxidation are well described by the spectral shape obtained after air exposure (i.e., the second topmost spectrum in Figure 1b, here labeled “ TiO_2 ” due to its agreement in line position with the reference value of 458.9 eV^{12,18}). Again, we subtract this spectrum with a suitable weight factor to give a feasible line shape for the residual spectrum (13% of the overall spectral intensity). The thus-derived difference spectrum is shown in black in the center of Figure 3, labeled “Difference”. Again, it is evident from the line shape that still more than one species contributes. Thus, (3) we have used the EA spectrum, representative of TiO_2 , and shifted it to the respective reference value positions for Ti_2O_3

(19) Scofield, J. H. *J. Electron Spectrosc. Relat. Phenom.* **1976**, *8*, 129–137.

(457.6 eV, labeled “Ti₂O₃”) and TiO (455.6 eV, labeled “TiO”).^{10,12} Again, suitable weight factors were applied (Ti₂O₃: 22% and TiO: 42% of the overall spectral intensity) to give a feasible line shape. The residual is shown as a black spectrum at the bottom of Figure 3 and labeled “Residual”. Clearly, two peaks with similar (spin–orbit) splitting to that for the EA spectrum are visible in the residual (15% of the overall spectral intensity). These cannot be accounted for by any of the previous Ti “species”, suggesting that this residual represents a further (fifth) Ti species, which we associate with Ti–C bonds, in agreement with the reference position for TiC_x compounds (454.6 eV¹¹). Note that the weight factors were independently corroborated by a simultaneous intensity fit using the parameters (line shape, width, position) derived from fits of the individual Ti and TiO₂ spectra (as well as for the shifted TiO₂ spectra that are used as “Ti₂O₃” and “TiO” spectra). Of course, the fit minimizes the χ^2 of the residual, which leads to statistically relevant deviations from the zero line, but naturally not to a representative (physically sound) spectral shape for an additional species. Thus, we consider the here-presented difference approach as the most reliable way to identify the presence of an additional species (the Ti–C species).

Figure 4 (lower half) shows that the oxidation of Ti as a function of time (in UHV) progresses toward higher Ti oxidation states. This is seen in the shift of spectral weight between the red (5 min) and purple (120 min) spectra and, even more visible, in the difference spectrum (120 min – 5 min; black, bottom of figure), as shown by the red arrows. With this trend and the assignments made above, we then interpret the oxidation process as a decrease of the number of Ti atoms in a metallic and a Ti–C bond environment and an increase of the number of Ti atoms in an oxygen-containing environment. Note that the here-described oxidation behavior of the Ti atoms in Ti–Ti and Ti–C bonds was derived for a very thin Ti coverage on the SWNTs. A thicker Ti deposition could potentially result in an increased number of Ti atoms in the Ti–C bond environment (i.e., at the interface with SWNTs) and an additional outer Ti layer, potentially reducing the relative contribution of oxidized Ti atoms. However, thicker Ti layers may also lead to a clustering of Ti atoms⁹ and are thus generally considered to be less effective for hydrogen storage.

Our results thus show that Ti adatoms on SWNT, even if deposited as (initially) metallic atoms, can easily be oxidized, even under UHV conditions. Consequently, the use of Ti-decorated carbon nanomaterials for hydrogen storage appears impossible, unless the natively formed Ti–O bonds can be broken and Ti can be liberated for adsorption of hydrogen molecules. We will show in the following that this approach becomes feasible using Li as a “liberation agent”.

It was previously reported that Li-decorated SWNTs also show potential for hydrogen storage.²⁰ However, due to the strong chemical reactivity of Li, similar oxidation problems (as reported here for Ti-decorated SWNTs) can be expected. Since the energy gain from the exothermal oxidation of Li to Li₂O

(heat of formation $\Delta H_f = -597.9$ kJ/mol at 298 K²¹) is larger than the energy needed for the endothermal reduction of TiO₂ to Ti₂O₃ or TiO ($\Delta H_f = 364$ and 483 kJ/mol at 298 K, respectively^{22,23}), we speculate that Li may be used to reduce the oxidation of Ti on SWNTs.

As mentioned in conjunction with Figure 1b, the deposition of Li on the EA-Ti/SWNT/Au sample induces pronounced spectral changes of the Ti 2p spectrum. This is seen in the upper half of Figure 4, which shows the Ti 2p spectrum for the EA-Ti/SWNT sample before and after Li deposition. As is clearly visible in the “Difference” spectrum (Li-EA), the spectral weight shifts back toward lower binding energy, contrary to what is found for the oxidation process in UHV (lower half of Figure 4). This indicates that the deposited Li reacts with oxygen of the previously formed TiO₂ layer, suggesting that it is possible to use Li as an “agent” to reduce the natively formed TiO₂ to lower oxidation states.

Note that we are not attempting to assign the Li-induced change in spectral weight to specific Ti species; this is due to the fact that the Li deposition induces a shift of all (other) core level lines to higher binding energies (not shown). The O 1s line shifts by 0.7 eV, while the C 1s line shifts by 0.3 eV. This is presumably due to a combination of effects, including chemical bonding (e.g., a Li–Ti–O complex^{14,15}) and changes of the local electrostatic environment of the probed atoms. It is very likely that the Ti 2p line is also shifted toward higher binding energies (by an amount on the order of 0.3–0.7 eV). Thus, an assignment to specific species is not attempted in this paper, while it is clearly evident that the Ti atoms are reduced by the Li deposition.

4. Conclusions

In conclusion, we have utilized X-ray photoelectron spectroscopy for the investigation of the chemical surface structure of Ti- and Li/Ti-decorated SWNTs. We find that the Ti adatoms on SWNT/Au oxidize, even under UHV conditions. The formation of the native titanium oxide on the surface of deposited Ti would hinder the interaction of Ti with H₂ molecules in hydrogen storage applications. The additional deposition of Li on (oxidized) Ti/SWNT/Au indicates that Li can possibly be used as an agent to reduce oxidized titanium and hence “liberate” Ti atoms for adsorption of hydrogen molecules. Given the relative simplicity of evaporating Li from a getter element, this could be used as a practical way for using metal-decorated carbon nanomaterials in hydrogen storage applications.

Acknowledgment. This work was supported by the U.S. Department of Energy through the UNLV FCAST program under Grant No. DE-FG36-05GO85028.

JA910976K

(21) Lide, D. R., Ed. *CRC Handbook of Chemistry and Physics*, 89th ed. (Internet Version); CRC Press/Taylor and Francis: Boca Raton, FL, 2009.

(22) Campbell, C. T. *Surf. Sci. Rep.* **1997**, *27*, 1–111.

(23) Diebold, U. *Surf. Sci. Rep.* **2003**, *48*, 53–229.

(20) Sun, Q.; Wang, Q.; Jena, P.; Kawazoe, Y. *J. Am. Chem. Soc.* **2005**, *127*, 14582.